Electronic Supplementary Material (ESI) for Journal of Materials Chemistry A.

Supporting Information

General strategy of decorating 3D carbon nanofiber aerogel derived from bacterial cellulose with nano-Fe_3O_4 for high-performance flexible and binder-free lithium-ion battery anodes

Yizao Wan,[ab] Zhiwei Yang,[b] Guangyao Xiong,*[a] and Honglin Luo*[b]

[a] *School of Mechanical and Electrical Engineering, East China Jiaotong University, Nanchang 330013, China*

[b] *School of Materials Science and Engineering, Tianjin Key Laboratory of Composite and Functional Materials, Key Laboratory of Advanced Ceramics and Machining Technology, Ministry of Education, Tianjin University, Tianjin 300072, China*

Corresponding authors.

E-mail addresses: xiongguangyao@163.com (G. Xiong), hlluotju@126.com (H. Luo)

Experimental section

Preparation of nano-Fe_2O_3-decorated BC aerogels

The preparation and cleaning procedures of BC pellicles were identical to those described in our previous work.[1] The resulting BC pellicles were freeze-dried in liquid nitrogen (-196 ºC) to obtain BC aerogels. The nano-Fe_2O_3-decorated BC aerogels were synthesized by the hydrothermal method. Typically, a BC aerogel ($25 \times 25 \times 1$ mm^3) was immersed in 50 mL of 0.05 M $Fe(NO_3)_3 \cdot 9H_2O$ aqueous solution for 48 h at room temperature. Next, the BC aerogel was immersed in 40 mL of 0.5 M urea aqueous solution under agitation, and subsequently transferred to a closed container at 120 °C for 10 h. The product was taken out and freeze-dried, resulting in a nano-Fe_2O_3-decorated BC aerogel, which was named as Fe_2O_3-BC-05. Other nano-Fe_2O_3-decorated BC aerogels were synthesized with the same procedure except that the concentration of $Fe(NO_3)_3 \cdot 9H_2O$ was different, namely 0.1 and 0.2 M. The resultant samples are denoted as Fe_2O_3-BC-10 and Fe_2O_3-BC-20, respectively.

Preparation of Fe_3O_4-BC-CNFs

The as-obtained Fe_2O_3-BC aerogels were carbonized in a tube furnace under nitrogen atmosphere. The samples were heated from room temperature to 300 ^{o}C at a heating rate of 1 °C min^{-1}, held for 1 h and then heated to 600 ^{o}C at 2 °C min^{-1}. The carbonization lasted for 2 h to yield Fe_3O_4-BC-CNFs (named as Fe_3O_4-BC-CNFs-x, corresponding to Fe_2O_3-BC-x, x=05, 10, 20).

Preparation of coin cells

To prepare working electrodes, BC-CNFs and Fe_3O_4-BC-CNFs were punched into circular samples with a diameter of 13 mm and vacuum dried at 100 ^oC for 12 h. The dried samples were directly used to assemble into cells without any additives or binders. For comparison, Fe_3O_4 nanoparticles (around 10 nm in size) obtained from Sinopharm Chemical Reagent Co., Ltd., Beijing, China, were used to prepare coin cells. Fe_3O_4 nanoparticles, carbon black, and polyvinylidene fluoride (PVDF) with a mass ratio of 80 : 10 : 10 were mixed into a homogeneous slurry using N-methyl-2-pyrrolidone (NMP) as the solvent. The slurry mixture was coated onto Cu foil followed by vacuum drying at 100 ^oC for 12 h. The coin cells (CR2032) were fabricated using metallic lithium as the counter electrode, porous polypropylene film (Celgard 2400) as the separator, and 1 M LiPF6 in ethylene carbonate (EC)–dimethyl carbonate (DMC)–ethylmethyl carbonate (EMC) (1 : 1 : 1 by volume) as the electrolyte. The cell assembly was carried out in an Ar-filled glovebox. Before all electrochemical measurements, cells were aged for 12 h.

Electrochemical measurements

Charge–discharge experiments were performed at a constant current density between 0.005 and 3 V (vs Li^+/Li) using a BTS-5V10mA battery tester. Cyclic voltammetry (CV) measurement was performed using a CHI 660B electrochemical workstation at 0.5 mV/s within the range of 0.0-3.0 V (vs Li^+/Li). For the electrochemical impedance spectroscopy (EIS) measurements, the excitation voltage applied to the cell was 5 mV and the frequency ranges from 0.01 Hz to 100 kHz.

Characterization

Samples were characterized by scanning electron microscopy (SEM, Nova Nanosem 430), transmission electron microscopy (TEM, Tecnai G2F-20), and X-ray diffraction (XRD, Rigaku D/Max 2500 v/pc) with Cu K_α radiation. Thermogravimetric analysis (TGA) was performed on a simultaneous TGA/DSC analyzer (STA449F3) from 30 to 800 °C at a heating rate of 10 °C/min in air. Fourier transformed infrared spectroscopy (FTIR) analysis was conducted by Shimadzu IRPrestige-21 (Japan) and FTIR spectra were recorded in a spectral range of 4000-400 cm^{-1} with a resolution of 4 cm^{-1}. Raman spectra were recorded by an RM2000 spectrometer (Renishaw Co.). XPS analysis was performed by an X-ray photoelectron spectrometer (Thermo ESCALAB 250Xi, Thermo Fisher Scientific Inc., Waltham, MA, USA). Conductivity measurements were carried out on a Keithley 2635 sourcemeter unit as previously reported.[2] Nitrogen adsorption isotherms and the Brunauer–Emett–Teller (BET) surface area of Fe_3O_4-BC-CNFs were measured at 77 K with a surface area analyzer (W-BK132F, Beijing JWGB Sci. & Tech., China).

Notes and references

1. Y. Z. Wan, Y. Huang, C. D. Yuan, S. Raman, Y. Zhu, H. J. Jiang, F. He and C. Gao, *Mater. Sci. Engin. C*, 2007, **27**, 855-864.
2. H. Si, H. Luo, G. Xiong, Z. Yang, R. S. Raman, R. Guo and Y. Wan, *Macromol. Rapid Commun.*, 2014, **35**, 1706-1711.

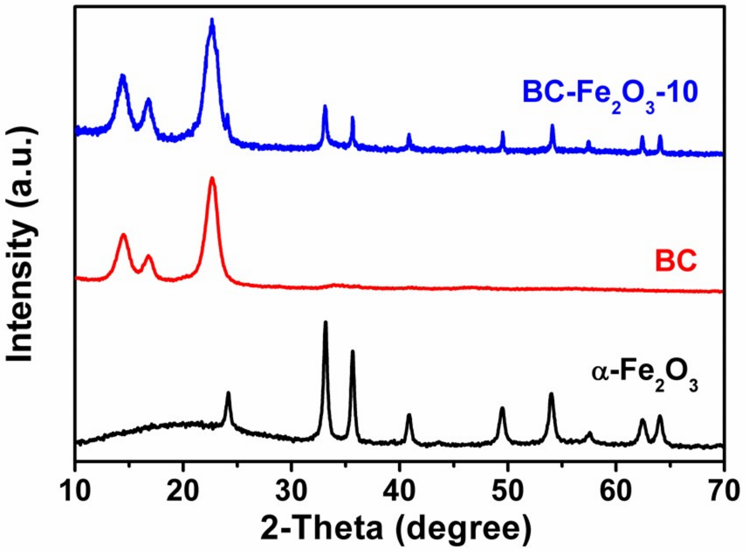

Fig. S1 The XRD patterns of α-Fe_2O_3, BC, and Fe_2O_3-BC-10.

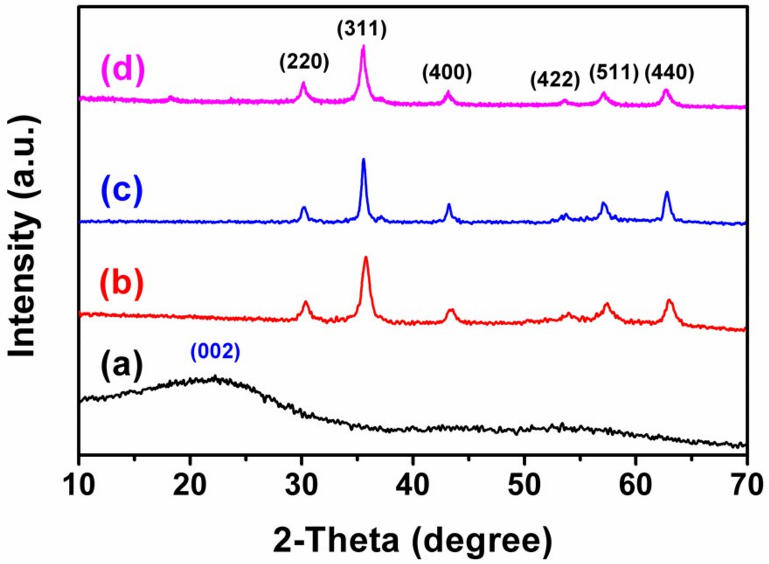

Fig. S2 XRD patterns of BC-CNFs (a), Fe_3O_4-BC-CNFs-05 (b), Fe_3O_4-BC-CNFs-10 (c), and Fe_3O_4-BC-CNFs-20 (d).

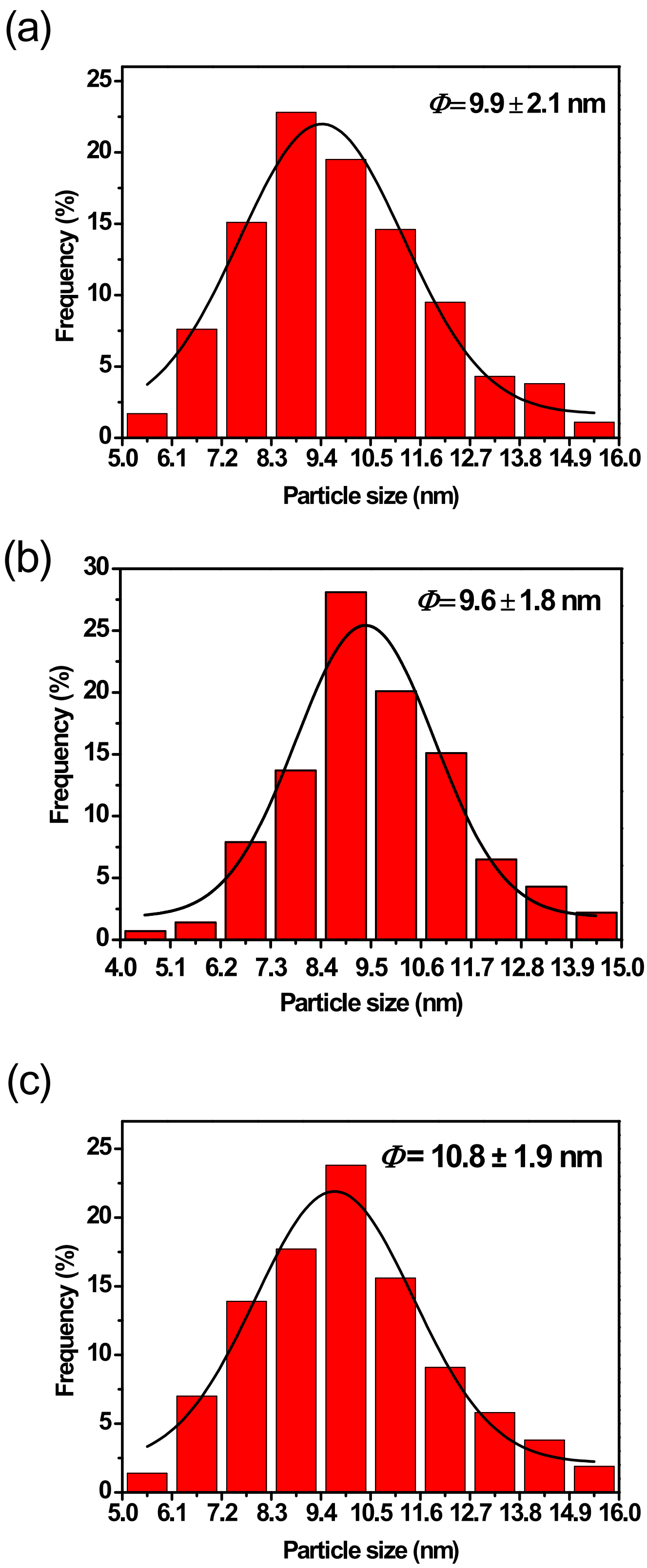

Fig. S3 Particle size distribution of Fe_3O_4 nanoparticles on the surface of Fe_3O_4-BC-CNFs-05 (a), Fe_3O_4-BC-CNFs-10 (b), and Fe_3O_4-BC-CNFs-20 (c) ($p > 0.05$ when any two materials are compared).

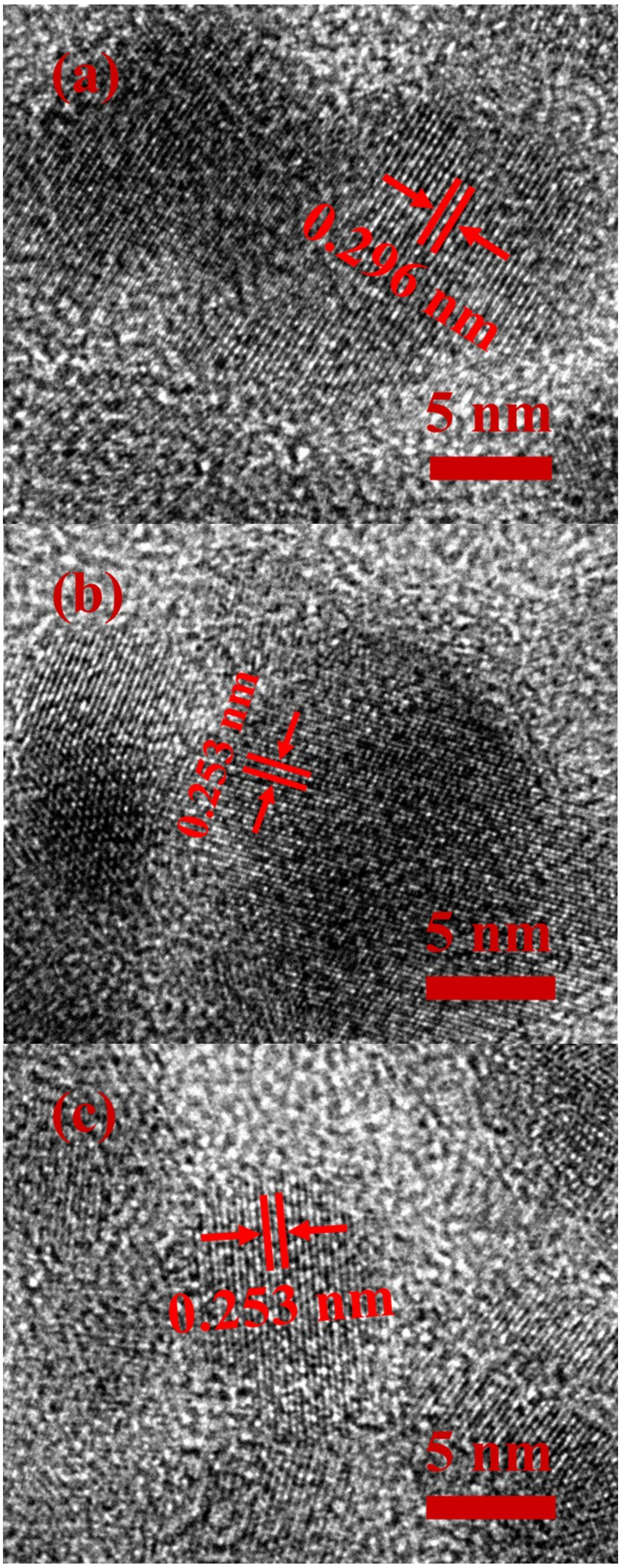

Fig. S4 HRTEM images of Fe_3O_4-BC-CNFs-05 (a), Fe_3O_4-BC-CNFs-10 (b), and Fe_3O_4-BC-CNFs-20, showing lattice fringe with a spacing of 0.253 nm.

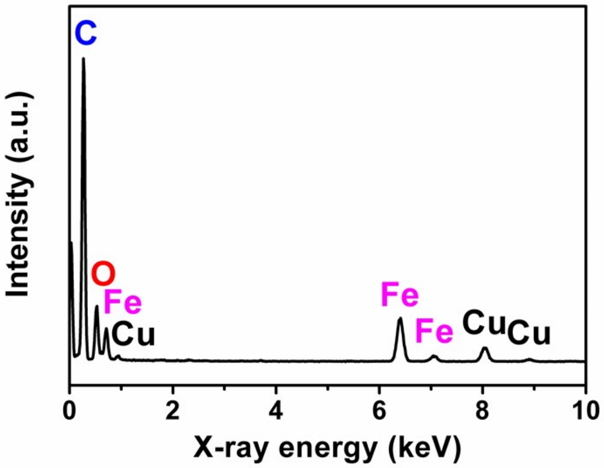

Fig. S5 EDX pattern of Fe_3O_4-BC-CNFs.

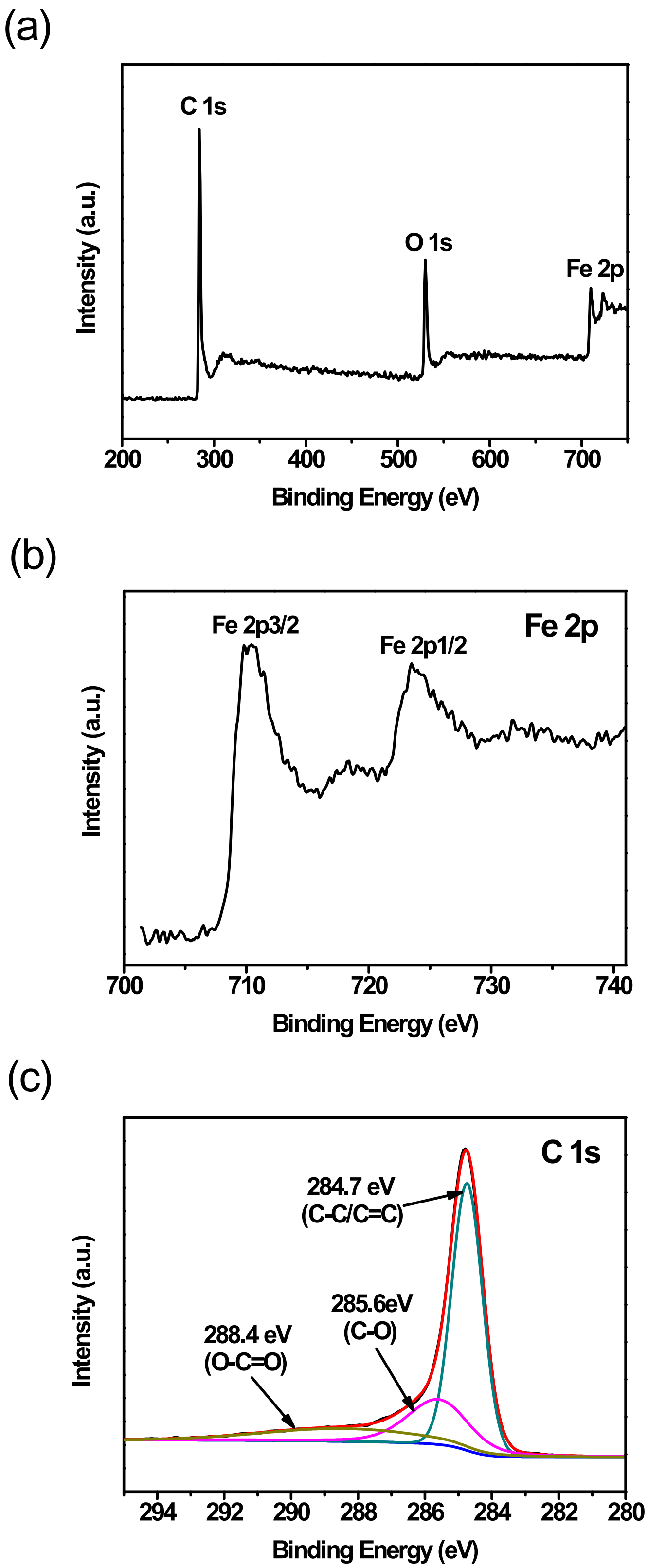

Fig. S6 X-ray photoelectron spectroscopy (XPS) spectra of wide scan (a), Fe 2p peaks (b), and C 1s peaks of Fe_3O_4-BC-CNFs.

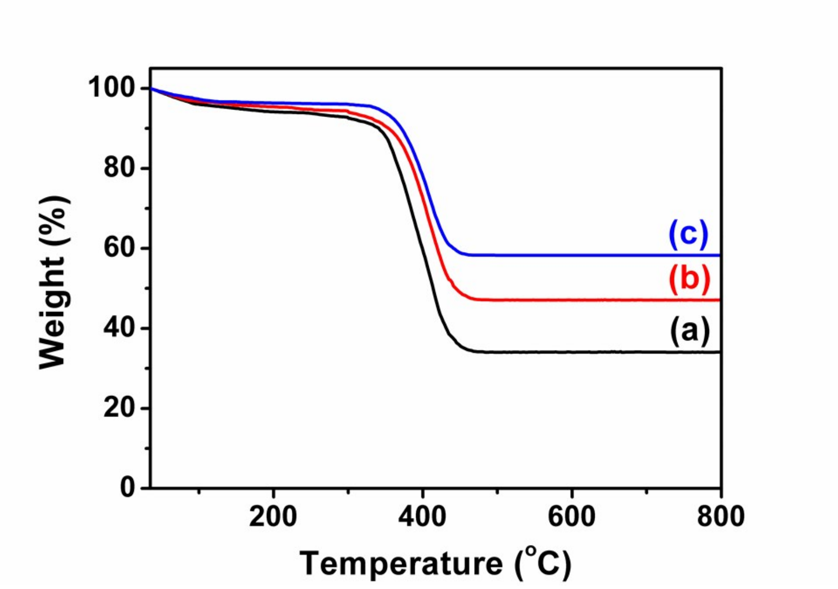

Fig. S7 TG curves of Fe_3O_4-BC-CNFs-05 (a), Fe_3O_4-BC-CNFs-10 (b), and Fe_3O_4-BC-CNFs-20 (c).

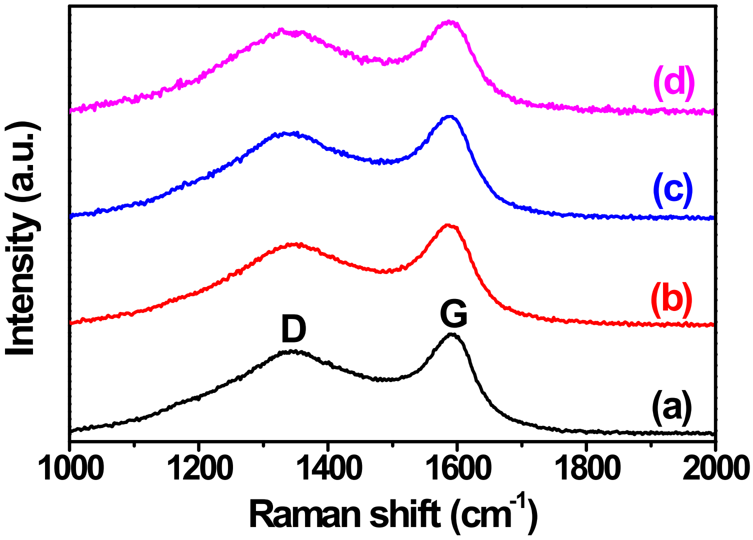

Fig. S8 Raman spectra of BC-CNFs (a), Fe_3O_4-BC-CNFs-05 (b), Fe_3O_4-BC-CNFs-10 (c), and Fe_3O_4-BC-CNFs-20 (d).

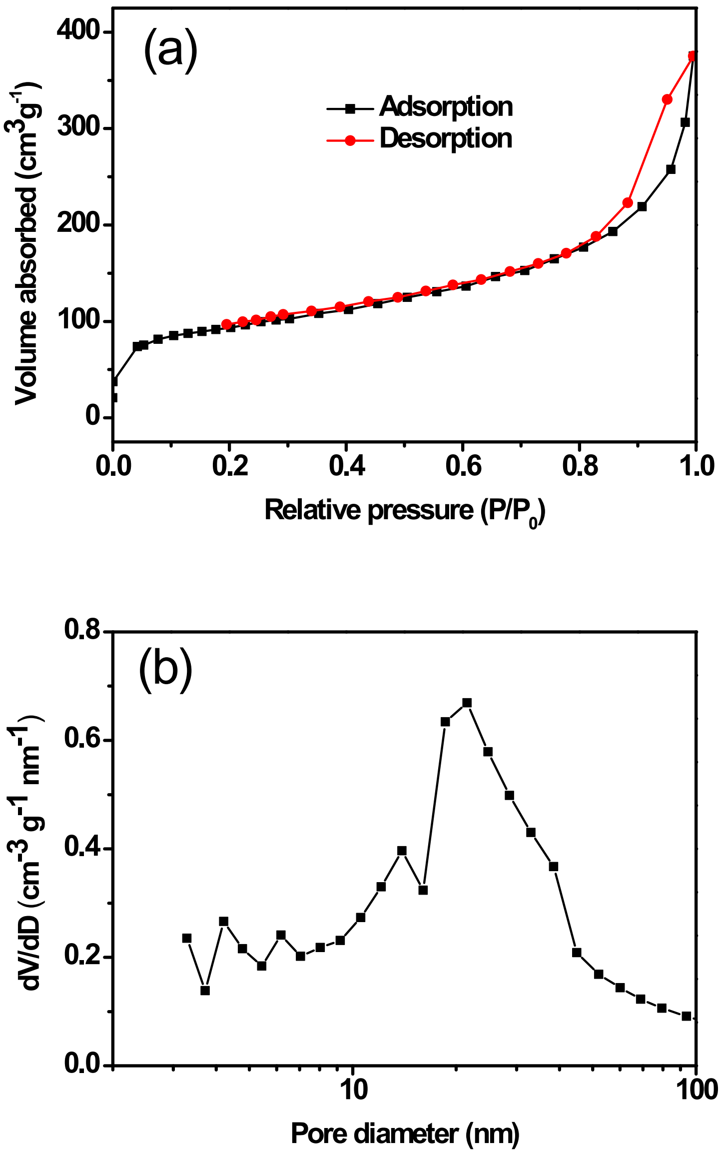

Fig. S9 Nitrogen adsorption and desorption isotherm (a) and pore-size distribution (b) of Fe_3O_4-BC-CNFs-10 (the Brunauer-Emmett-Teller specific surface area was calculated to be 322 m^2 g^{-1}).

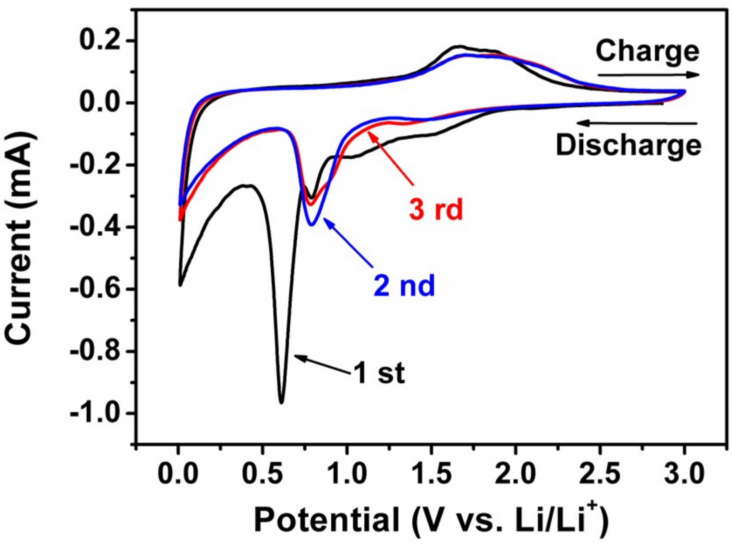

Fig. S10 Cyclic voltammetry (CV) curves of Fe_3O_4-BC-CNFs during the first three cycles.

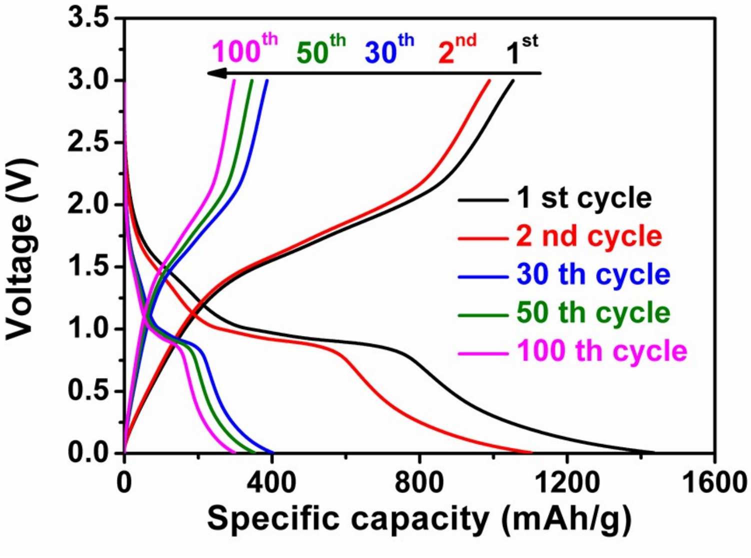

Fig. S11 Discharge/charge profiles of bare Fe_3O_4 nanoparticles.

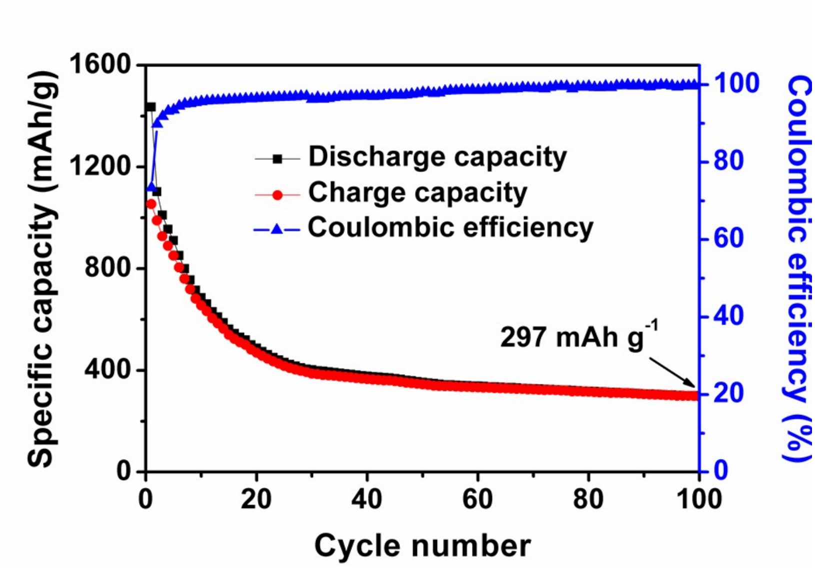

Fig. S12 Charge and discharge capacities with Coulombic efficiency as a function of cycle number of bare Fe_3O_4 nanoparticles at a current density 100 mA g^{-1}.

Table S1 *R* values of bare BC-CNFs and Fe_3O_4-BC-CNFs.

Samples	D peak (cm^{-1})	G peak (cm^{-1})	*R*
Bare BC-CNFs	1342	1590	0.80
Fe_3O_4-BC-CNFs-05	1339	1589	0.81
Fe_3O_4-BC-CNFs-10	1338	1588	0.85
Fe_3O_4-BC-CNFs-20	1329	1587	0.88

Table S2 Relevant parameters of Fe_3O_4-BC-CNFs-10 and bare Fe_3O_4 under different conditions.

Samples	Conditions	R_f (Ω)	R_{ct} (Ω)
Fe_3O_4-BC-CNFs-10	Before rate performance tests	23.0	136.2
	After rate performance tests	8.6	106.3
Bare Fe_3O_4	Before rate performance tests	39.8	361.9